Ao *et al. Environmental Sciences Europe* (2024) 36:69
https://doi.org/10.1186/s12302-024-00887-9

Environmental Sciences Europe

RESEARCH

Open Access

Ecological risk assessment and source tracing of heavy metals in surface sediments of a hilly riverine reservoir in Chongqing, China

Liang Ao[1*], Ruiting Chang[1], Yanqiu Tang[1] and Sheng Zhang[1]

Abstract

Background This work conducted quantitative and qualitative analyses on the heavy metals in 32 surface sediment samples collected from eight sampling sites across four seasons in the Yutan reservoir, a typical mountainous hilly riverine reservoir in Southwest China.

Results Nine heavy metals were identified: (Cr, Cd, Pb, Cu, Zn, Hg, As, Ni, and Co). The concentrations varied within the ranges of 23.16 ~ 34.62, 0.53 ~ 1.09, 31.88 ~ 59.04, 51.94 ~ 85.84, 106.76 ~ 227.69, 0.08 ~ 0.15, 12.57 ~ 25.60, 12.06 ~ 27.64 and 11.04 ~ 14.56 mg/kg, respectively, following a decreased concentration order of Zn > Cu > Pb > Cr > Ni > As > Co > Cd > Hg. Except for Cd, which accumulated in winter, and Hg, which reduced in spring. The concentration of heavy metals showed no significant seasonal variation and generally had higher contents at the river mouth and lower concentrations in open water areas and branches. The geoaccumulation index (I_{geo}) assessment also indicated that the reservoir was uncontaminated by Cr and Ni ($I_{geo} < 0$), slightly polluted by Pb, Cu, Zn, and Co ($0 < I_{geo} < 1$), moderately polluted by Hg and As ($1 < I_{geo} < 2$), and heavily polluted by Cd ($1.44 < I_{geo} < 2.48$). Notably, the most polluted sites were at the river mouth, followed by the sediments in branches with slight pollution. Source tracing analysis revealed that Cr, Ni, Cd, Pb, Hg, As, organic matter, total nitrogen, and total phosphorus were primarily attributed to non-point sources. In contrast, Fe was linked to the hardware industry. Moreover, Al originated from sewage and drinking water treatment processes. Cu and Zn were discharged from three components, indicating complex sources.

Conclusions The findings underscored that non-point sources were the primary contributors to the increased risk of heavy metal contamination in the reservior's sediment. In addition, to effectively manage the risk and enhance the aquatic environment, greater focus should be placed on the inner load of heavy metals in the sediment of the mountainous hilly riverine reservoirs, particularly after controlling external pollution sources.

Keywords Sediment, Heavy metal assessment, Sources distinguished, Reservoir, Mountainous hilly riverine reservoirs

*Correspondence:
Liang Ao
aoliang77777@163.com
[1] Chongqing Academy of Eco-Environmental Science, Southwest Branch of Chinese Research Academy of Environmental Sciences, Chongqing 400700, China

Background

Heavy metal contamination has emerged as a significant focus in aquatic environmental protection, such as in the Yutan Reservoir, a prominent hilly riverine ecosystem in southwest China [1]. Sediments are a sink of pollutants, including heavy metals, in aquatic environments due to their toxicity, persistence, and bioaccumulation potential effection [1, 2]. As the physicochemical conditions at the sediment–water interface change, the heavy metals are released back into the water, acting as a source of pollutants [2, 3]. Hence, the occurrence of heavy metals in both sediment and water poses significant threats to the aquatic ecosystem and even human health through exposure to biota, such as phytoplankton, benthic invertebrates, fishes, and waterbirds, while also exacerbating these risks through their enrichment in trophic levels [4–6].

Assessing ecological risks resulting from heavy metals in sediments in hilly riverine reservoir environments, such as the Yutan Reservoir, requires tailored approaches [7, 8]. Geochemical approaches and multivariate statistical analysis, including sediment pollution index (SPI) factor analysis (FA), factor analysis–multiple linear regression analysis (FA–MLR), and geoaccumulation index (I_{geo}), are widely used for identifying pollution sources and quantifying their contributions [9–11]. Moreover, changes in environmental conditions or physical and biological disturbances can cause the dynamic of heavy metals in water and sediment [12]. Consequently, factors such as water temperature, pH value, and dissolved oxygen (DO) can accelerate the release process, particularly under anaerobic conditions [13]. Furthermore, in river ecosystems, the heavy metal input from upstream can accumulate in sediments and be released under stagnant, anaerobic, and low pH conditions of the slow-flowing reaches.

The Yutan Reservoir was constructed in 1958 and expanded later in 2011. It is a typical mountain riverine reservoir that sustains over one million people in the northwest of Chongqing. It faces significant pollution challenges from sewage, industrial wastewater, and non-point sources in the upper reach, which numerous metal processing plants compound. Environmental challenges, however, have been a significant concern. Prior to the 2010s, the lack of wastewater treatment facilities led to serious water pollution, with most of the wastewater being discharged directly into the lake [14]. Since then, water pollution control policies have been implemented, focusing on reducing heavy metal contamination and improving water quality, and it has shown significant improvement in recent years [14].

To this end, this study hypothesizes that the heavy metal concentrations in sediments of the Yutan Reservoir fluctuate seasonally. In addition, anthropogenic sources could be the major contributor to the heavy metal pollution. Therefore, the SPI, I_{geo}, FA, and FA–MLR were applied to assess heavy metal pollution over the four seasons. Notably, the findings will contribute to a better understanding of reservoir protection and contribute to the aquatic ecosystem conservation strategies in mountainous riverine reservoirs.

Materials and methods

Study area

The Yutan Reservoir is located in the Dazu district of Chongqing, ranging from E105°40′22.68" ~ 105°43′57.39", N29°32′34.97" ~ 29°35′3.55". It lies in the lower reaches of the Laixi River and Kulong River, serving as a crucial tributary in the upper reaches of the Yangtze River. The reservoir has a storage capacity of 149.6 million m^3 and covers a surface water area of 22.35 km^2. In addition, the Laixi River, flowing through the Dazu District, has an average annual flow of 7.32 m^3/s and stretches 72 km, while the Kulong River's flow was 2.74 m^3/s. Furthermore, the Chengdu–Chongqing region experiences a subtropical moist climate, with an annual average temperature of 17.3 ℃, peaking at 39.8 ℃ in July and dropping to 1 ℃ in January.

As the largest artificial lake in western Chongqing, Yutan Reservoir plays a vital role in the development of local society, especially in the Chengdu–Chongqing economic region, which is the growth pole in Western China. While a noticeable difference has been made to the environment, the lingering effects of heavy metal accumulation continue to pose persistent toxic harm to the aquatic ecosystem.

Sediment samples collection

Sediment samples were collected from eight different locations across the Yutan reservoir throughout the four seasons of 2015 (Fig. 1). In each area and season, four sampling sites were randomly selected. Open water areas covering all sample sites represented the quality of the whole reservoir. At each site, five sediment samples were collected from the top 20 cm of sediment. The samples were mixed and well-homogenized to form a composite sample for each site. To preserve sample integrity, all samples were immediately sealed in plastic bags and stored at 4 ℃ for transportation, and then were freeze-dried in the laboratory. The water quality at these sites was monitored monthly under the guidelines of the Chinese national standard (GB3838-2002), including temperature, pH, SD, DO, Chla, F, S, Cl, SO_4^{2-} and suspended solid (SS). The primary software used for statistical analysis is Stata 17.0, and Origin 2022 is utilized for graphing.

Sample analytical methods

The freeze-dried sediment samples were meticulously sieved through a 100 μm mesh via a mortar prior to the analyses of the concentrations of heavy metals (Cr, Cd, Pb, Cu, Zn, Ni, Co, Fe, and Al), organic matter (OM), total phosphorus (TP), and total nitrogen (TN).

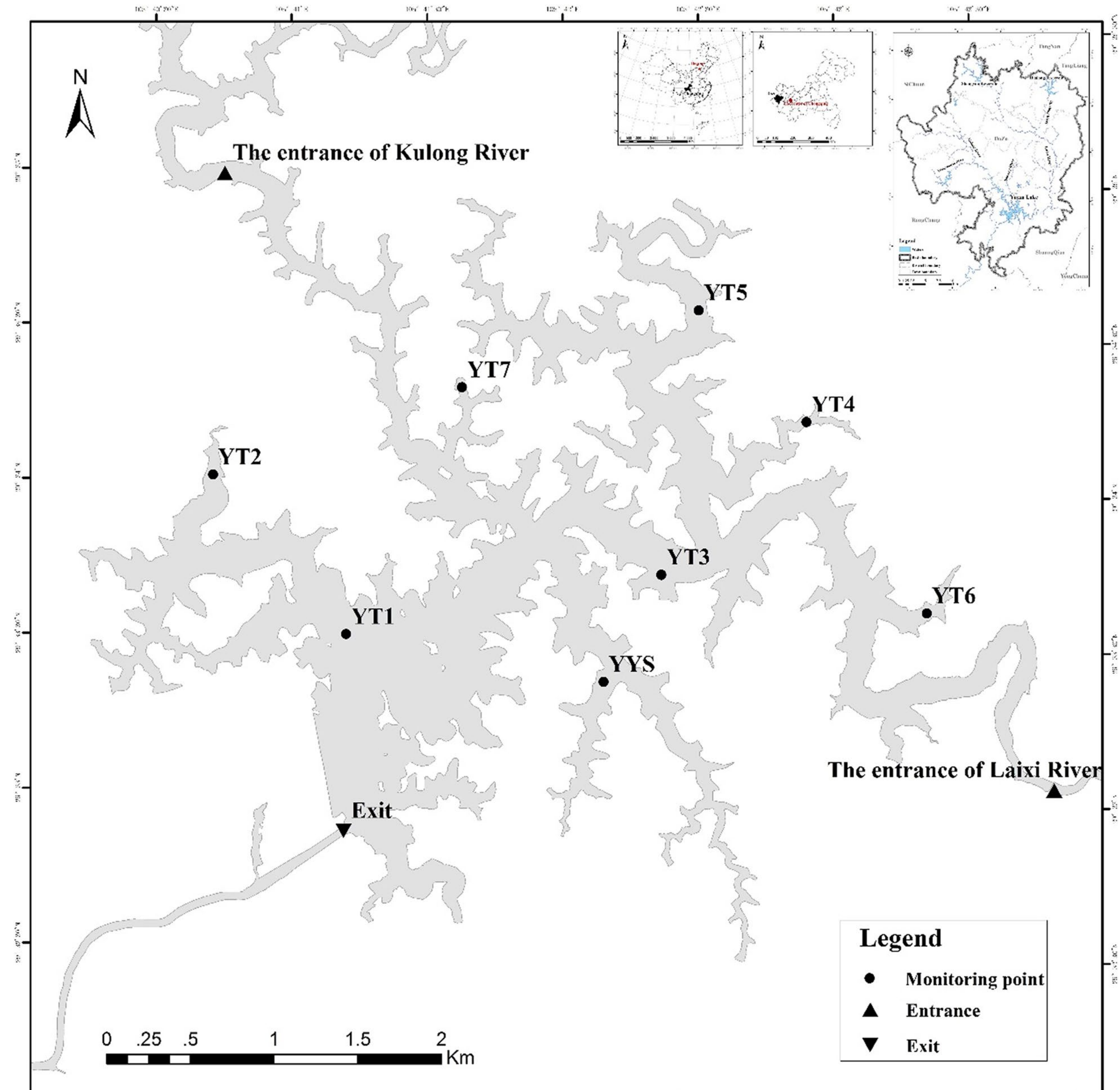

Fig. 1 Location of sampling sites distribution in the Yutan Reservoir, Chongqing (YYS was named YT8 in the water quality monitor)

OM was determined via titration with $FeSO_4$ following digestion with $K_2Cr_2O_7$–H_2SO_4 solution. TP sediments were qualified through the digestion of sediments with HF–$HClO_4$. Moreover, TN was detected by using the alkaline potassium persulfate digestion method.

Regarding heavy metal analysis, the total sediment digestion was performed in Teflon vessels following the classical open digestion procedures involving a mixture of concentrated HF–$HClO_4$–HNO_3. Concentrations of heavy metals (Cr, Cu, Zn Ni, Co, Fe, and Al) in solution were measured using inductively coupled plasma optical emission spectrometry (ICP–OES).

The Cd and Pb levels were detected by inductively coupled plasma mass spectrometry (ICP–MS). The As and Hg concentrations were determined by atomic fluorescence spectrometry (AFS) and cold atomic absorption (CAA), respectively.

All the analytical procedures and the data thus obtained complied with the standards of the China Inspection

Body and Laboratory Mandatory Approval (CMA) to ensure the reliability and credibility of the measurements.

Data analysis

I_{geo} was first introduced by Müller in 1979 and has been widely adopted as a quantitative measure of assessing heavy metal pollution in aquatic sediments [15]. The formula for I_{geo} is expressed as follows:

$$I_{geo} = \log_2\left(C_n / 1.5B_n\right) \tag{1}$$

In the equation for I_{geo}, C_n is the measured concentration of a particular metal. Simultaneously, B_n is the background value of this metal in local sediments (as detailed in Table 1). Factor 1.5 is the background matrix correlation factor due to lithogenic variation [16].

I_{geo} is categorized into seven classes to indicate varying degrees of pollution, providing a clear and structured means to assess the extent of heavy metal pollution in aquatic sediment samples, from unpolluted to extremely polluted:

Unpolluted, $I_{geo} < 0$; unpolluted to moderately polluted, $0 \le I_{geo} < 1$; moderately polluted, $1 \le I_{geo} < 2$; moderately to heavily polluted, $2 \le I_{geo} < 3$; heavily polluted, $3 \le I_{geo} < 4$; heavily to extremely polluted, $4 \le I_{geo} < 5$; extremely polluted, $I_{geo} \ge 5$.

The SPI is a comprehensive tool for assessing sediment quality with respect to heavy metal concentrations and their associated metal toxicity (T_f). In this risk assessment framework, Fe and Al are not considered toxic heavy metals. Moreover, the toxicity factors (T_f) are assigned as Zn for a weight of 1, Cr, Ni, and Co for a weight of 2, Pb and Cu for a weight of 5, As for a weight of 10, and Cd and Hg for a weight of 40.

The formula of SPI can be expressed as follows:

$$SPI = \sum\left(C_n / B_n \times T_f\right) \Big/ \sum T_f \tag{2}$$

In the equation for the SPI, C_n is the measurement of metal concentration, while B_n is the background value of local sediment for metals (Table 1).

SPI is categorized into five classes to indicate varying degrees of pollution, from natural to dangerous levels:

Natural, SPI < 2; low polluted, 2 ≤ SPI < 5; moderately polluted, 5 ≤ SPI < 10; highly polluted, 10 ≤ SPI < 20; dangerous, SPI > 20.

Two-way analysis of variance (two-way ANOVA), Pearson's correlation analysis (PCA), factor analysis (FA), and factor analysis–multiple linear regression (FA–MLR) were employed by stata17 to elucidate the interrelationships among these heavy metals and to identify common pollution sources, both natural and anthropogenic, within the basin.

Results and discussion

Concentrations of heavy metals in surface sediment

Surface sediments of the Yutan Reservoir revealed the presence of nine heavy metals, including Cr, Cd, Pb, Cu, Zn, Hg, As, Ni, and Co (Fig. 2). Besides the concentrations of Cr and Ni, Yutan's average concentrations of Cd, Pb, Cu, Zn, Hg, and As exceed background values 87.6%, 39.4%, 57.7%, 62.8%, 70.64%, 81.15% and 140.34%, respectively, presented in Additional file 1. Separately, summary statistics across different sites are presented in Additional file 2. It is worth noting that concentrations generally decreased from the river mouth to open water to branches, suggesting external inputs as a significant source. Notably, Pb levels were consistently higher at the river mouth across all seasons, with marked seasonal spikes—autumn for open waters and winter for branches—potentially indicative of the non-point source. Mercury (Hg), with an average concentration 70.64% higher than the background value, aligns with precipitation patterns that peaked in summer and reached a minimum in winter combined with higher concentrations at the river mouth. In addition, the average rainfall recorded the highest amount of rainfall in summer, while the lowest one was recorded in winter. Above all, this pattern suggests that mercury accumulation is influenced by water input and might be caused by the fine particles solid spread in these seasons and settling to the bottom, which requires more time.

Ordered by seasons, the summary statistics (mean, standard deviation (SD), maximum (Max), minimum values (Min), standard deviation (SD), and coefficient of variation (CV) of nine heavy metals are presented in Additional file 3.

Based on the above data, it was found that the concentrations of Cr, Ni, and Co did not vary significantly with seasonal variations. Cr showed prominent accumulation in open water areas with the lowest concentration in the branch, which was located far away from the river mouth in summer and autumn. In winter and spring, Cr in the

Table 1 Heavy metals background contents (Bn) of sediment in the Yangtze River of the Three Gorges Reservoir reaches

Heavy metals	Cr	Cd	Pb	Cu	Zn	Hg	As	Co	Ni
B_n(mg·kg^{-1})	78.03	0.13	23.88	25	69.88	0.036	5.84	5.58	29.47

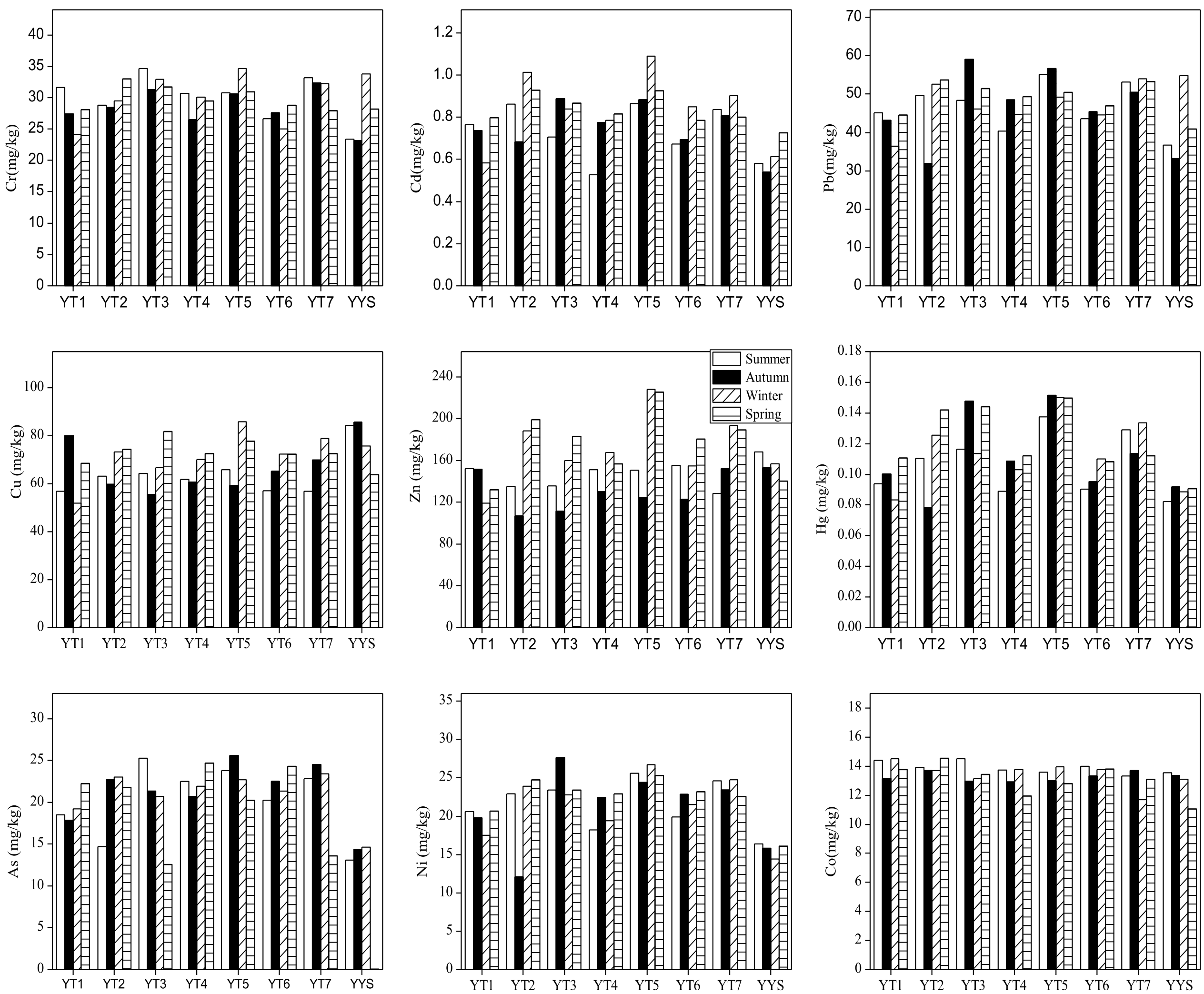

Fig. 2 Heavy metals' distribution in Yutan Lake

branch also had an apparent increase in sediment, which may have been affected by the inner water cycle.

Ni showed apparent changes in different sample sites, and it had a higher concentration in the river mouth and a lower concentration in open water areas and branches. Cu did not show significant changes in the four seasons, but dramatic differences appeared in different sites. In summer and autumn, the highest concentration appeared in the branches, with the lowest concentration in the river mouth. When it came to winter and spring, the highest concentration appeared in open-water areas. These findings suggested that Cu might travel with runoff input, and as it ran into the wet season, the concentration of Cu increased in the river mouth, which might have followed the suspended solid (SS) input.

Zn had a noticeable increase in winter and spring, which was about 1.5 times compared to other seasons. Notably, the river mouth acted as a hotspot during the colder months. As such, this seasonal accumulation could be attributed to increased runoff and sediment transport during wet seasons. This hypothesis is supported by similar studies in riverine systems, which suggest that during the rainy season, heavy metals tend to be desorbed and released from the surface of particulate matter into the overlying water. Moreover, the proportion of heavy metal residues increases [16]. Furthermore, Co did not show a significant difference in timescale, is likely due to the natural effect. The stable distribution suggests natural sources, whereas Cd displayed a winter accumulation followed by a spring decline.

Seasonal and location analysis: two-way ANOVA

Skewness–Kurtosis test results (Additional file 4) demonstrate that the data do not significantly deviate from a normal distribution and can meet the normality assumption required by most statistical analysis methods. The results of two-way ANOVA applied to the nine heavy metals are shown in Additional file 5.

According to the two-way ANOVA results, significant effects are observed for Cd concentrations at sampling points 2, 5, and 7, with the summer season also showing a substantial influence. In the case of Cr concentrations, sampling points 3, 5, and 7 are significantly impactful, while seasonal variations do not exhibit any significant effect. Pb concentrations are affected considerably by sampling points 3, 5, and 7, with no notable seasonal influence. In addition, Cu concentrations are significantly influenced by sampling point 8, with the summer season also playing a significant role. Zn concentrations also show a notable effect at sampling point 5, and both summer and autumn seasons have a considerable impact. Hg concentrations are significantly affected at sampling points 2, 3, 5, and 7, with the summer season again having a significant influence. Moreover, As and Ni concentrations display significant effects at sampling points 3, 5, 7, and 8, but no seasonal variation shows a significant impact. Lastly, Co concentration is notably influenced by sampling points 4, 7, and 8, with the summer season also showing a significant effect. Furthermore, it's vital to notice that the constant for each metal regression result is the most significant besides the location and the seasons.

Pollution assessment

I_{geo} was calculated to assess the sediment pollution (Table 2). In all seasons, I_{geo} for Cr and Ni were below

Table 2 I_{geo} distribution in different seasons of Yutan Lake

Number	Seasons	I_{Cr}	I_{Cd}	I_{Pb}	I_{Cu}	I_{Zn}	I_{Hg}	I_{As}	I_{Ni}	I_{Co}
YT1	Spring	− 2.06	2.03	0.31	0.87	0.33	1.04	1.13	− 1.09	0.72
YT2	Spring	− 1.83	2.25	0.58	0.99	0.93	1.39	1.39	− 0.84	0.80
YT3	Spring	− 1.88	2.15	0.52	1.12	0.80	1.42	1.24	− 0.92	0.68
YT4	Spring	− 1.99	2.07	0.46	0.95	0.58	1.05	1.32	− 0.95	0.51
YT5	Spring	− 1.92	2.25	0.49	1.05	1.10	1.47	1.37	− 0.80	0.61
YT6	Spring	− 2.02	2.01	0.39	0.95	0.78	1.00	1.28	− 0.93	0.72
YT7	Spring	− 2.07	2.04	0.57	0.95	0.85	1.05	1.42	− 0.97	0.65
YYS	Spring	− 2.05	1.90	0.19	0.77	0.42	0.75	0.74	− 1.46	0.40
YT1	Summer	− 1.89	1.97	0.33	0.60	0.54	0.80	1.16	− 1.10	0.78
YT2	Summer	− 2.02	2.14	0.47	0.75	0.37	1.03	1.34	− 0.95	0.73
YT3	Summer	− 1.76	1.86	0.43	0.78	0.37	1.11	1.32	− 0.92	0.79
YT4	Summer	− 1.93	1.44	0.17	0.72	0.53	0.72	0.52	− 1.28	0.71
YT5	Summer	− 1.93	2.15	0.62	0.81	0.52	1.35	1.49	− 0.79	0.70
YT6	Summer	− 2.14	1.78	0.28	0.60	0.57	0.74	1.21	− 1.15	0.74
YT7	Summer	− 1.82	2.10	0.57	0.60	0.30	1.26	1.47	− 0.84	0.67
YYS	Summer	− 2.32	1.58	0.03	1.17	0.68	0.61	0.64	− 1.43	0.69
YT1	Autumn	− 2.10	1.92	0.27	1.09	0.53	0.89	1.08	− 1.16	0.65
YT2	Autumn	− 2.04	1.81	− 0.17	0.67	0.03	0.54	0.75	− 1.87	0.71
YT3	Autumn	− 1.90	2.19	0.72	0.57	0.09	1.45	1.53	− 0.68	0.63
YT4	Autumn	− 2.14	1.99	0.44	0.69	0.31	1.01	1.36	− 0.98	0.63
YT5	Autumn	− 1.94	2.18	0.66	0.66	0.25	1.49	1.44	− 0.86	0.63
YT6	Autumn	− 2.08	1.83	0.34	0.80	0.23	0.82	1.21	− 0.95	0.67
YT7	Autumn	− 1.86	2.05	0.49	0.90	0.54	1.07	1.38	− 0.92	0.71
YYS	Autumn	− 2.34	1.47	-0.11	1.19	0.55	0.76	0.58	− 1.48	0.68
YT1	Winter	− 2.28	1.58	0.02	0.47	0.18	0.63	1.03	− 1.33	0.80
YT2	Winter	− 1.99	2.38	0.56	0.96	0.84	1.22	1.37	− 0.89	0.71
YT3	Winter	− 1.83	2.11	0.36	0.83	0.61	1.07	1.28	− 0.96	0.65
YT4	Winter	− 1.96	2.01	0.32	0.90	0.67	0.93	1.24	− 1.19	0.72
YT5	Winter	− 1.76	2.48	0.46	1.19	1.12	1.48	1.55	− 0.73	0.74
YT6	Winter	− 2.23	2.12	0.31	0.95	0.56	1.03	1.36	− 1.04	0.72
YT7	Winter	− 1.86	2.21	0.59	1.07	0.88	1.31	1.48	− 0.84	0.48
YYS	Winter	− 1.79	1.65	0.61	1.01	0.58	0.71	0.71	− 1.62	0.65

0, with different variations in each site, indicating the unpolluted states of Cr and Ni. In addition, Pb, Cu, Zn, and Co were found in unpolluted to moderately polluted states ($0 < I_{geo} < 1$), with a few sites having higher pollution ($I_{Cu} > 1$). Pb had a higher accumulation in winter and spring but a lower accumulation in summer and autumn. The river mouth had the most accumulation among the three sites. Pb in open water had a more obvious accumulation than in branches, with the highest average value of 0.56. Accumulation of Cu was relatively stable, with only a tiny increase in spring and winter. In contrast, the open water and river mouth had a lower accumulation than in branches, which suggested that Cu might travel as the inner cycle in this reservoir. The accumulated state of Cu was transferred, and the highest value of ICu reached 1.03. The seasonal change of Zn indicated its prominent accumulation in winter and spring. Zn was more polluted in summer and autumn, with the value of I_{Zn} almost twice as much as in other spring and winter seasons. The spatial difference provided a clear answer for the apparent pollution in the river mouth, with an average value reaching 0.75. This could be observed with Co. The seasonal variation of Co was limited, but it had the most obvious accumulation in open water areas, with the I_{CO} values ranging from 0.65 to 0.80. Hg and As were moderately polluted with I_{geo} and varied from 1 to 2. No noticeable seasonal changes were found for Hg or As. Spatial differences of Hg showed the accumulation in the river mouth with values mostly above 1.40. However, no dramatic changes were found in branches and open water in any season, with moderate pollution in all seasons (I_{Hg} ranged from 0 to 1). Notably, the open water and river mouth were polluted with $I_{As} > 1$. However, the branches might not be directly affected by the external load, leading to I_{As} values between 0 and 1. Furthermore, Cd was the most polluted heavy metal, with I_{Cd} varying from 1.44 to 2.48, suggesting moderately polluted ($1 \leq I_{geo} < 2$) or moderately to heavily polluted ($2 \leq I_{geo} < 3$) in different sites. The variation of Cd did not show a significant difference in the four seasons, which its established source might cause. The river mouth areas showed heavier pollution than in open water, with a slight difference in branches, with I_{Cd} reaching 2.25.

The SPI was applied to examine the potential risk of sediment in the four seasons (Fig. 3). Results from most of these sediments suggested low polluted states. The most polluted site was observed in the river mouth, with the value reaching 5.46, suggesting a moderately polluted state in the river mouth. The lowest value of SPI was observed in branches with a value of 2.92. The results showed that there were no noticeable differences between each season. Consequently, this indicated that it sustained a low polluted state. The polluted areas were mainly from the river mouth, followed by the open water areas. The cleanest area was branches that were far away from the river mouth. Overall, the sediment of Yutan Reservoir mostly sustained low or moderate pollution. Thus, more attention should be paid to the accumulation of heavy metals in the food chain in the reservoir.

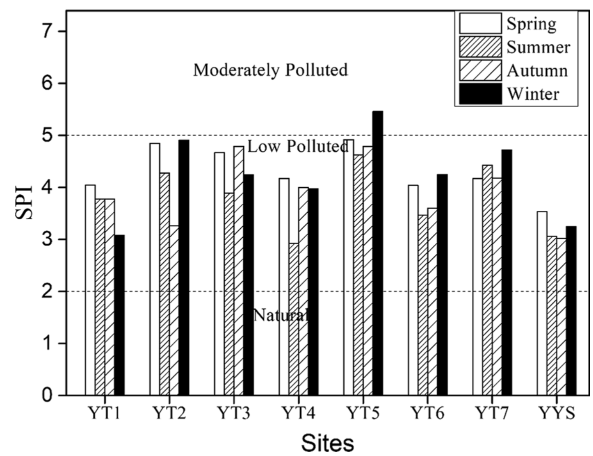

Fig. 3 Sediment pollution index (SPI) in the sediment of Yutan Lake

Heavy metals sources tracing

To identify the source of heavy metals, seasonal differences of several factors as well as their relationship with heavy metal concentration were considered, including physical and chemical properties of the water body (ORP, moisture, pH, and bulk density) and concentrations of nutrients (OM, TP, and TN). Heavy metals and these noted factors were also analyzed with Pearson correlation and factor analysis to track their sources. Our results showed that the pH varied in a range of 7.32 ~ 7.96. It changed little with the seasonal switch but displays the highest value in branches in summer and the lowest value in open water in spring. The sediment bulk density and ORP ranged from 0.69 ~ 0.80 g/cm^3 and 78 ~ 138 mV, respectively. Most of the ORP was under 200 mV, indicating the facultative state of these sediments. In this case, the heavy metals might not be stable and could be readily released into the water body [17]. The average sediment moisture was 80%, with the highest value (88%) found in open water areas in summer and the lowest one in branches in winter. The difference in moisture between summer and winter indicated that the moisture of sediments was dramatically affected by seasons and locations that were closely related to rainfall. OM varied in an extensive range of 6.35 ~ 57.22 g/kg. The sediment in spring contained the highest organic matter content, possibly due to the algae growth and death accumulation in this season. This also suggested that the rivers and branches of the reservoir had a higher OM than the open water. Notably, the OM of the river mouth's sediment had the highest amount of organic matter due to the input from the river. The OM in the sediment was further removed in the open water, leading to relatively low concentrations. The TN of the sediment had an average value of 0.88 g/kg with a range from 0.25 g/kg to 1.33 g/kg. The spring's sediment still had the highest concentration from the whole year, and the TN doubled in the river mouth compared to the branches.

The average concentration of P in the sediment was 0.94 mg/kg (0.62 – 1.36 mg/kg), which was higher than that in other reservoirs. More P concentration was found in spring and little in summer, with a slight increase in winter. The P in open water and branches were less than those in the river mouth. Notably, this was closely associated with the P inputs in the upper river. The average concentration of Fe was 12.15 g/kg (9.46–16.07 g/kg), and there was no significant change among seasons. The lowest concentration was found in the branches, while the river mouth had the highest concentration of Fe. The concentration of Al varied from 4.69 to 11.76 g/kg (average of 7.85 g/kg). Higher concentrations of Fe were found in winter. Nevertheless, no dramatic spatial differences were found in the sampling sites, suggesting the background sources with relatively stable levels.

Results from the correlation analysis are shown in Additional file materials. During the whole year, the concentrations of Cr, Cd, Pb, Hg, As, and Ni were closely correlated with each other, indicating a similar source of these heavy metals in the studied area. The relevance among other heavy metals was poor. In addition, the concentrations of Cr, Cd, Pb, Hg, As, and Ni were significantly associated with OM, TN, and TP. The nutrients were probably from human activities, such as urban sewage and agricultural fertilizer, from upper reach, including the Dazu district. Notably, the Dazu district has a high population and a well-developed agriculture concentration of Zn, which was significantly correlated with the concentration of OM, TN, Cd, Cu, Hg, and Fe. Moreover, the pH value was negatively correlated with the concentrations of Cd and Zn. With the decrease in pH values, Cd and Zn might be released from the sediments, posting relevant risks to the water quality.

The FA was also used to track the sources of heavy metals. Three factors were found to have a total variance of 77% (Table 3). Factor 1 was closely associated with heavy metals, with an eigenvalue of 4.836 and a cumulative percentage of 43.97%. Cu, Zn, and Fe mainly contributed Factor 2 with an eigenvalue of 1.968 and a cumulative percentage of 61.85%. Cu, Zn, Co, and Al mainly contributed to factor 3. Generally, Factor 1 explained the source of Cr, Cd, Pb, Hg, As, and Ni, while Fe and Al were merely from Factor 2 and 3, respectively. It is also worth noting that Cu and Zn had relatively high scores in all three factors, suggesting various sources of Cu and Zn in the studied areas. The bold number shows the mainly contributed factor for the high weight.

Table 3 FA and heavy metal sources identified in the sediment of the Yutan Lake

Variables	Factor 1	Factor 2	Factor 3
Cr	**0.659**	− 0.132	0.006
Cd	**0.908**	0.012	0.088
Pb	**0.867**	− 0.131	− 0.211
Cu	0.178	**0.78**	**0.458**
Zn	**0.501**	**0.61**	**0.501**
Hg	**0.933**	− 0.025	− 0.04
As	**0.89**	− 0.271	− 0.038
Ni	**0.916**	− 0.194	− 0.015
Co	− 0.099	− 0.482	**0.59**
Fe	0.173	**0.743**	− 0.291
Al	− 0.045	− 0.24	**0.851**
Eigenvalues	4.836	1.968	1.674
Percent of variance (%)	43.967	17.886	15.218
Cumulative percentage (%)	43.967	61.853	77.071

Bold values show the mainly contributed factor for the high weight

The I_{geo} results of factor analysis–multiple linear regression analysis (FA–MLR) as follows: I_{geo}(Cd) = 0.232 factor_score1 + 0.012 factor_score2 + 0.01 factor_score3 + 1.991, meanwhile, Factor1 and constant shows significant ($p < 0.01$), which confirms that Factor 1 was closely associated with heavy metals. The results for other metals are illustrated in Table 4.

I_{geo} of Cr and Ni are smaller than 0, indicating the accumulation originated primarily from background supply, such as sediment weathering, soil erosion, etc. In contrast, the more positive I_{geo} of Cd, Pb, Hg, and As indicated apparent human input of them with a moderately to heavy pollution status in the Yutai Reservoir. As shown in previous research, nutrients in the water were mainly from non-point sources, and they might accumulate in sediment with the water flowing down. From the FA in this study, Factor 1 could be attributed to non-point sources from the upper river, mainly from the diffused pollution sources such as soil erosion, leaching of pesticides and fertilizers, aquaculture tail water, etc. Factor 2 could mainly explain Fe and partially explain Cu and Zn. Longshui Town has a hardware industry, with iron products supplements, which could be an industry source of Fe [18]. There were also 14 sewage treatment facilities in the region of upper reach, with a total treatment capacity of 77,170 tons per day. The first-class A and B standards for the pollutant discharge for urban sewage treatment

Table 4 Factor analysis–multiple linear regression analysis (FA–MLR) and heavy metals sources identified in the sediment of the Yutan Lake

Linear regression							
I_{Cd}	**Coef**	**St. Err**	***t* value**	***p* value**	**[95% Conf.**	**Interval]**	**Sig**
factor_score1	0.232	0.019	11.90	0	0.192	0.272	***
factor_score2	0.012	0.021	0.57	0.572	-0.031	0.055	
factor_score3	0.01	0.023	0.43	0.67	-0.037	0.057	
Constant	1.991	0.019	105.57	0	1.952	2.029	***
Mean dependent var		1.991		SD dependent var		0.250	
R-squared		0.836		Number of obs		32	
F test		47.530		Prob > *F*		0.000	
Akaike crit. (AIC)		− 48.695		Bayesian crit. (BIC)		− 42.832	
Linear regression							
I_{Cr}	**Coef**	**St.Err**	***t* value**	***p* value**	**[95% Conf.**	**Interval]**	**Sig**
factor_score1	0.101	0.019	5.43	0	0.063	0.139	***
factor_score2	− 0.017	0.02	− 0.84	0.408	− 0.058	0.024	
factor_score3	− 0.091	0.022	− 4.16	0	− 0.136	-0.046	***
Constant	− 1.992	0.018	− 110.70	0	− 2.028	− 1.955	***
Mean dependent var		− 1.992		SD dependent var		0.157	
R-squared		0.620		Number of obs		32	
F test		15.218		Prob > *F*		0.000	
Akaike crit. (AIC)		− 51.704		Bayesian crit. (BIC)		− 45.841	
Linear regression							
I_{Pb}	**Coef**	**St.Err**	***t* value**	***p* value**	**[95% Conf.**	**Interval]**	**Sig**
factor_score1	0.196	0.014	14.35	0	0.168	0.224	***
factor_score2	− 0.036	0.015	− 2.43	0.022	− 0.066	− 0.006	**
factor_score3	− 0.091	0.016	− 5.67	0	− 0.124	− 0.058	***
Constant	0.384	0.013	29.10	0	0.357	0.411	***
Mean dependent var		0.384		SD dependent var		0.218	
R-squared		0.895		Number of obs		32	
F test		79.222		Prob > *F*		0.000	
Akaike crit. (AIC)		− 71.578		Bayesian crit. (BIC)		− 65.716	
Linear regression							
I_{Cu}	**Coef**	**St.Err**	***t* value**	***p* value**	**[95% Conf.**	**Interval]**	**Sig**
factor_score1	0.033	0.012	2.66	0.013	0.008	0.058	**
factor_score2	0.202	0.013	15.04	0	0.174	0.229	***
factor_score3	0.021	0.015	1.43	0.165	− 0.009	0.051	
Constant	0.863	0.012	72.14	0	0.839	0.888	***
Mean dependent var		0.863		SD dependent var		0.196	
R-squared		0.893		Number of obs		32	
F test		77.661		Prob > *F*		0.000	
Akaike crit. (AIC)		− 77.782		Bayesian crit. (BIC)		− 71.919	
Linear regression							
I_{Zn}	**Coef**	**St.Err**	***t* value**	***p* value**	**[95% Conf.**	**Interval]**	**Sig**
factor_score1	0.122	0.02	5.99	0	0.08	0.164	***
factor_score2	0.241	0.022	10.89	0	0.195	0.286	***
factor_score3	0.035	0.024	1.47	0.154	− 0.014	0.084	

Table 4 (continued)

Linear regression							
I_{Zn}	**Coef**	**St.Err**	***t* value**	***p* value**	**[95% Conf.**	**Interval]**	**Sig**
Constant	0.551	0.02	27.94	0	0.511	0.592	***
Mean dependent var		0.551		SD dependent var		0.271	
R-squared		0.846		Number of obs		32	
F test		51.420		Prob > *F*		0.000	
Akaike crit. (AIC)		− 45.791		Bayesian crit. (BIC)		− 39.928	
Linear regression							
I_{Hg}	**Coef**	**St. Err**	***t* value**	***p* value**	**[95% Conf.**	**Interval]**	**Sig**
factor_score1	0.273	0.017	15.74	0	0.237	0.308	***
factor_score2	0.012	0.019	0.63	0.536	− 0.027	0.05	
factor_score3	− 0.024	0.02	− 1.17	0.253	− 0.066	0.018	
Constant	1.037	0.017	61.93	0	1.003	1.072	***
Mean dependent var		1.037		SD dependent var		0.283	
R-squared		0.899		Number of obs		32	
F test		82.803		Prob > *F*		0.000	
Akaike crit. (AIC)		− 56.263		Bayesian crit. (BIC)		− 50.400	
Linear regression							
I_{As}	**Coef**	**St.Err**	***t* value**	***p* value**	**[95% Conf.**	**Interval]**	**Sig**
factor_score1	0.268	0.009	28.29	0	0.249	0.287	***
factor_score2	− 0.085	0.01	− 8.24	0	− 0.106	− 0.064	***
factor_score3	0.092	0.011	8.21	0	0.069	0.114	***
Constant	1.2	0.009	130.88	0	1.181	1.218	***
Mean dependent var		1.200		SD dependent var		0.294	
R-squared		0.972		Number of obs		32	
F test		322.846		Prob > *F*		0.000	
Akaike crit. (AIC)		− 94.860		Bayesian crit. (BIC)		− 88.997	
Linear regression							
I_{Ni}	**Coef**	**St.Err**	***t* value**	***p* value**	**[95% Conf.**	**Interval]**	**Sig**
factor_score1	0.254	0.016	15.44	0	0.221	0.288	***
factor_score2	− 0.036	0.018	− 2.03	0.052	− 0.073	0	*
factor_score3	0.068	0.019	3.49	0.002	0.028	0.108	***
Constant	− 1.06	0.016	− 66.50	0	− 1.093	− 1.027	***
Mean dependent var		− 1.060		SD dependent var		0.275	
R-squared		0.903		Number of obs		32	
F test		86.873		Prob > *F*		0.000	
Akaike crit. (AIC)		− 59.449		Bayesian crit. (BIC)		− 53.587	
Linear regression							
I_{Co}	**Coef**	**St.Err**	***t* value**	***p* value**	**[95% Conf.**	**Interval]**	**Sig**
factor_score1	− 0.007	0.016	− 0.48	0.638	− 0.039	0.025	
factor_score2	− 0.013	0.017	− 0.74	0.465	− 0.047	0.022	
factor_score3	0.033	0.018	1.78	0.085	− 0.005	0.071	*
Constant	0.678	0.015	44.82	0	0.647	0.708	***
Mean dependent var		0.678		SD dependent var		0.087	
R-squared		0.127		Number of obs		32	
F test		1.354		Prob > *F*		0.277	

Table 4 (continued)

Linear regression							
I_{Co}	Coef	St.Err	*t* value	*p* value	[95% Conf.	Interval]	Sig
Akaike crit. (AIC)		− 62.851		Bayesian crit. (BIC)		− 56.988	

***$p < 0.01$

**$p < 0.05$

*$p < 0.1$

plants were applied in those sewage treatment facilities, resulting in the decreased concentration of TP from 1.20 mg/L in the influent to 0.295 mg/L in the effluent. In regards to the techniques used in sewage treatment facilities, phosphorus removal mainly depended on the use of chemicals, especially aluminum preparations, such as polymeric ferric aluminum sulfate, PAC, etc. Moreover, drinking water treatment also needs a large amount of Al with tailwater directly discharged into the reservoir (i.e., daily consumption of over 10 tons per day). Therefore, Factor 3 could explain not only Cu and Zn but also Co and Al from sewage and drinking water treatment. Overall, Cr, Ni, Cd, Pb, Hg, As, OM, TN, and TP were mainly from the non-point source, accompanied by flushed fertilizer. Furthermore, Fe was from the hardware industry, and Al came from sewage and drinking water treatment. Cu and Zn were supplied with more complicated sources.

Conclusions

In the current study, heavy metals varied significantly in spatial scale and in different periods, which demonstrated higher pollution in the open water and the river mouth than in branches. All sediments of the Yutan Reservoir mostly sustained low or moderate pollution. According to the geo-accumulation index, Cr and Ni were not polluted. Pb, Cu, Zn, and Co were determined as unpolluted to moderately polluted states. Hg and As were moderately polluted. The most polluted heavy metal was Cd. Heavy metal pollution is mainly concentrated in the river mouth. The open water area was the secondary pollution state. The cleanest area appeared in branches, which were far away from the river mouth. With sources distinguished, Cr, Ni, Cd, Pb, Hg, As, OM, TN, and TP were mainly attributed to non-point sources, which were accompanied by flushed fertilizer. The hardware industry likely contributed to Fe. Furthermore, Al came from sewage and drinking water treatment. The three components supplied Cu and Zn, indicating complicated sources, the sediment transport and accumulation during wet seasons may contribute to it.

Abbreviations

AFS	Atomic fluorescence spectrometry
Bn	Background contents
CAA	Cold atomic absorption
CMA	China inspection body and laboratory mandatory approval
DO	Dissolved oxygen
FA	Factor analysis
FA–MLR	Factor analysis–multiple linear regression analysis
ICP–MS	Inductively coupled plasma mass spectrometry
ICP–OES	Inductively coupled plasma optical emission spectrometry
Igeo	Geoaccumulation index
OM	Organic matter
SPI	Sediment pollution index
SS	Suspended solid
TN	Total nitrogen
TP	Total phosphorus

Supplementary Information

The online version contains supplementary material available at https://doi.org/10.1186/s12302-024-00887-9.

Additional file 1: Summary statistics for each metal in all sampling sites and seasons.

Additional file 2: Summary statistics for each metal by sampling points.

Additional file 3: Summary statistics for each metal by season.

Additional file 4: Skewness-Kurtosis test results.

Additional file 5: Two-way ANOVA applied to the nine heavy metal test results.

Author contributions

Liang Ao: data collection and analysis, writing—original draft preparation. Ruiting Chang: data analysis and revision. Yanqiu Tang: data collection. shen zhang: supervision, writing—review and editing.

Funding

This study was financially supported by the water pollution comprehensive control model under the background of the Three Gorges Reservoir Operation (2017YFC0404702) and Integrated research and engineering demonstration of typical urban water comprehensive treatment technology (cstc2015shms–ztzx20002).

Availability of data and materials

The datasets used and/or analyzed during the current study are available from the corresponding author upon reasonable request.

Declarations

Ethics approval and consent to participate

Not applicable.

Consent for publication
All authors agreed to publish this paper.

Competing interests
The authors declare that they have no competing interests.

Received: 31 December 2023 Accepted: 16 March 2024
Published online: 03 April 2024

References

1. Varol M (2011) Assessment of heavy metal contamination in sediments of the Tigris River (Turkey) using pollution indices and multivariate statistical techniques. J Hazard Mater 195:355–364. https://doi.org/10.1016/j.jhazmat.2011.08.051
2. Liang A, Wang Y, Guo H et al (2015) Assessment of pollution and identification of sources of heavy metals in the sediments of Changshou Lake in a branch of the Three Gorges Reservoir. Environ Sci Pollut Res 22:16067–16076. https://doi.org/10.1007/s11356-015-4825-8
3. Bere T, Dalu T, Mwedzi T (2016) Detecting the impact of heavy metal contaminated sediment on benthic macroinvertebrate communities in tropical streams. Sci Total Environ 572:147–156. https://doi.org/10.1016/j.scitotenv.2016.07.204
4. Rahman MS, Saha N, Molla AH, Al-Reza SM (2014) Assessment of anthropogenic influence on heavy metals contamination in the aquatic ecosystem components: water, sediment, and fish. Soil Sediment Contam Int J 23:353–373. https://doi.org/10.1080/15320383.2014.829025
5. Salman J, Hassan F, Abdulameer S (2015) A study on the fate of some heavy metals in water and sediments in lotic ecosystems. Int J Chem Phys Sci 4:36–45
6. Zhang L, Shao H (2013) Heavy metal pollution in sediments from aquatic ecosystems in China. Clean: Soil, Air, Water. https://doi.org/10.1002/clen.201200565
7. Qiao M, Ji H, Zhu X, Chen Y (2013) Fraction distribution and risk assessment of heavy metal in sediments of miyun reservoir. J Agro-Environ Sci 32:1423–1431
8. Loska K, Wiechuła D (2003) Application of principal component analysis for the estimation of source of heavy metal contamination in surface sediments from the Rybnik Reservoir. Chemosphere 51:723–733. https://doi.org/10.1016/S0045-6535(03)00187-5
9. Lin C, He M, Liu X et al (2013) Distribution and contamination assessment of toxic trace elements in sediment of the Daliao River System, China. Environ Earth Sci 70:3163–3173. https://doi.org/10.1007/s12665-013-2382-3
10. Ogbeibu AE, Omoigberale MO, Ezenwa IM et al (2014) Using pollution load index and geoaccumulation index for the assessment of heavy metal pollution and sediment quality of the Benin River Nigeria. Nat Environ 2:1. https://doi.org/10.12966/ne.05.01.2014
11. Ye C, Li S, Zhang Y, Zhang Q (2011) Assessing soil heavy metal pollution in the water-level-fluctuation zone of the three gorges reservoir, China. J Hazard Mater 191:366–372. https://doi.org/10.1016/j.jhazmat.2011.04.090
12. Hill NA, King CK, Perrett LA, Johnston EL (2009) Contaminated suspended sediments toxic to an Antarctic filter feeder: aqueous—and particulate-phase effects. Environ Toxicol Chem 28:409–417. https://doi.org/10.1897/08-328.1
13. Weiner S, Addadi L (2011) Crystallization pathways in biomineralization. Annu Rev Mater Res 41:21–40. https://doi.org/10.1146/annurev-matsci-062910-095803
14. Chongqing Dazu District Government (2013) the overall implementation plan for the ecological and environmental protection of Yutan Lake in Chongqing.
15. Chen W, Tan SK, Tay JH (1996) Distribution, fractional composition and release of sediment-bound heavy metals in tropical reservoirs. Water Air Soil Pollut 92:273–287. https://doi.org/10.1007/BF00283563
16. Cibic T, Franzo A, Celussi M, Fabbro C (2012) Benthic ecosystem functioning in hydrocarbon and heavy-metal contamined sediments of an Adriatic lagoon. Prog Ser 458:69–87. https://doi.org/10.3354/meps09741
17. Zhou M, Liao B, Shu W et al (2015) Pollution Assessment and potential sources of heavy metals in agricultural soils around Four Pb/Zn mines of Shaoguan City, China. Soil Sediment Contam Int J 24:76–89. https://doi.org/10.1080/15320383.2014.914152
18. (2022) Notice of Chongqing municipal development and reform commission on the announcement of the List of Chongqing Characteristic Towns for the Year 2022. In: Chongqing Dev. Reform Comm. https://fzggw.cq.gov.cn/zwxx/tzgg/202203/t20220302_10451732.html. Accessed 3 Mar 2024

Publisher's Note